

Computational fluid dynamic simulation to assess flow characteristics of an in vitro aneurysm model

D A Lott,^{1,2,3,4,5} M Siegel,⁵ H R Chaudhry,^{1,2,3,4,6} C J Prestigiacomo^{6,7,8}

¹Department of Mathematics, Applied Mathematics Research Center, Delaware State University, Dover, Delaware, USA

²Department of Biological Sciences, Applied Mathematics Research Center, Delaware State University, Dover, Delaware, USA

³Department of Applied Mathematics and

Theoretical Physics, Applied Mathematics Research Center, Delaware State University, Dover, Delaware, USA

⁴War-Related Illness and Injury

Center, VA Medical Center, East Orange, New Jersey, USA
⁵Department of Mathematical Sciences, Center for Applied Mathematics and Statistics, New Jersey Institute of Technology, Newark, New Jersey, USA
⁶Department of Biomedical Engineering, New Jersey Institute of Technology, Newark, New Jersey, USA

⁷Department of Neurological Surgery, New Jersey Medical School, University of Medicine and Dentistry of New Jersey, Newark, New Jersey, USA

⁸Department of Radiology, New Jersey Medical School,

University of Medicine and

Dentistry of New Jersey, Newark, New Jersey, USA

⁹Received 31 March 2009

Revised 7 August 2009

Accepted 10 August 2009

ABSTRACT

Background Modifications of in vitro aneurysm modeling to study the effects of morphology on flow dynamics are time consuming, costly and analysis tends to be more qualitative than quantitative. This study develops a virtual two-dimensional flow model replicating an in vitro aneurysm model and analyzes how changes in morphology modify flow characteristics.

Methods Using finite volume analysis, a two-dimensional saccular aneurysm model was created with a configuration matching a published, experimental, in vitro model. Qualitative comparisons were made determining whether a two-dimensional fluid dynamic model can replicate the results of an in vitro model. Quantitative changes in flow patterns, wall shear stress, dynamic pressure and maximum velocities were assessed by modifying the shape of the neck and proximal dome without modifying the overall size of the aneurysm.

Results A two-dimensional computational fluid dynamic model reproducing the shape of a published aneurysm demonstrated excellent qualitative fidelity to an in vitro flow model. Additional information regarding dynamic pressure, shear stress and velocity along the aneurysm neck and within the aneurysm dome were determined. Although all dimensions were kept constant, slight modifications of the neck and proximal dome resulted in quantitative changes in studied parameters, such as wall shear stress and dynamic pressure.

Conclusions Computer generated aneurysm flow models, when carefully developed, reproduce flow events within in vitro aneurysms providing objective data on biophysical parameters. Effective flow modeling of aneurysms depends on flow input, size of the parent vessel and aneurysm, and other factors. These data suggest that neck and proximal dome configuration, independent of size, are important characteristics of flow.

parameters (such as wall shear stress and dynamic pressure) to the development, growth and potential rupture of these lesions.^{1–7} Such analyses have included a broad spectrum of methodologies from actual bench top experimental models, virtual computer generated finite volume analysis models and the study and development of biomathematical equations describing flow phenomena.^{8–16} Although aneurysm size and location seem to be correlated with aneurysmal rupture, other characteristics of aneurysms such as aspect ratio, shape and location may also contribute.¹⁷

Computer simulation models for aneurysm development, growth and rupture are quite helpful in providing a relatively low cost alternative to bench top modeling yet they have been criticized because they lack experimental validation.¹⁸ Current approaches include the use of computational fluid dynamics (CFD) and biomorphometric techniques which combine three-dimensional x ray angiography and CFD.^{19–25}

In order to determine whether carefully constructed computer simulation models can truly mimic in vitro aneurysm models and their results, a commercial state of the art computer program designed for modeling fluid flow in complex geometries was used to solve the Navier–Stokes equations of an independently published in vitro experimental model of a side wall aneurysm.⁹ Direct comparisons of the flow signatures for the virtual and experimental model were then made to assess the validity of the computer generated side wall aneurysm. Additionally, while maintaining a constant neck size, the effects of variations in the configuration of the aneurysm neck and proximal dome were assessed with respect to wall shear stress, dynamic pressures, flow velocities and flow signatures.

MATERIALS AND METHODS

Construction of two-dimensional computer flow model

Blood flow in the principle conducting arteries (such as arteries comprising the circle of Willis) is governed by the Navier–Stokes equation²⁶

$$\frac{\partial v}{\partial t} + (v \cdot \nabla)v = F_g - \frac{1}{\rho} \nabla P + \frac{\mu}{\rho} \nabla^2 v \quad (1)$$

where v is fluid velocity, F_g represents gravitational or body forces, P is pressure, ρ is fluid density and μ is fluid viscosity.

The model for our study simulates an internal carotid artery, measuring 3.6 mm in diameter with a lateral wall aneurysm of neck width of 3.1 mm, a dome diameter of 5.3 mm and height of 5.3 mm.

The formation, growth and potential rupture of a cerebral aneurysm is dependent on a myriad of factors which include congenital weaknesses in certain layers of the parent vessel, the biological response of tissues to stress, mechanical (flow related) stressors and genetics. Among the many biophysical factors, arterial pressure, shear stress and the direct effects of dynamic pressure on the vessel wall play an important role in the formation and growth of cerebral aneurysms. Consequently, progress in understanding the natural history of aneurysm is hampered by the complex interaction of these factors and the inability to adequately study these lesions *in vivo*.

Although somewhat limited, the in vitro study of cerebral aneurysms has been helpful in assessing the relative contribution of different biophysical

The model was scaled by a factor of 5 and all studies were performed on a two-dimensional fluid dynamics model with a Newtonian, non-compressible fluid. The use of Newtonian fluids is appropriate in this setting as it replicated the *in vitro* conditions of the published experimental model. No-slip boundary conditions, representing no flow at the interface between the wall of the model and the fluid, were assumed throughout the model, again in order to replicate bench top conditions.

The computational domain and grid were created using the commercial computer program GAMBIT (Fluent Incorporated, V.2.4.6; Lebanon, New Hampshire, USA), capable of meshing complex geometries in two and three dimensions. Once the domain (model) and its mesh were developed to precisely match the *in vitro* model, the computational geometry was imported into a commercially available software package, FLUENT (Fluent Incorporated, V.6.3.26), for analysis of velocity, dynamic pressure and shear stress distributions along the parent vessel and within the aneurysm. Very intricate user defined functions were created to simulate the velocity profile depicted in the experimental model (figure 1). Computations were performed on a Silicon Graphics Fuel, R10000 processor, Unix Version 6.5.22.

Numerical analysis and validation

FLUENT software uses a finite volume approach to solve equations satisfying conservation of mass and momentum, displacement, velocity and wall shear stress.²⁷ All simulations were performed in two dimensions, with double precision. For the full aneurysm, 4760 quadrilateral cells were utilized, subject to a minimum face area of $4.80 \times 10^{-5} \text{ m}^2$ and a maximum face area of $1.88 \times 10^{-4} \text{ m}^2$. The pulsatile flow conditions imposed on this virtual model were identical to those of an *in vitro* model¹⁷ that used a saturated solution of sodium thiocyanate with density, $\rho = 1287 \text{ kg/m}^3$ and viscosity $\mu = 4.4 \times 10^{-3} \text{ N/m}^2$, flowing through the silicon resin model. Initial operating conditions were set to zero atmospheric pressure. Simulations were calculated by imposing an inlet boundary condition on the right boundary and outflow conditions on the left boundary, thus making the flow direction right to left. This convention was chosen to match the velocity profile of the bench model.

Figure 1 Inlet velocity boundary profile on the left boundary of the artery. The pulsatile profile is approximated by a fast Fourier transform to fit the intra-aneurysmal velocity field of the flow cycle.⁹ Note the pulsatile pattern of flow reflecting the flow profile seen in arteries of the circle of Willis. Time points at which all tabulated results were obtained are identified: (a) $t=0.05$, early flow acceleration; (b) $t=0.15$, intermediate flow acceleration; (c) $t=0.225$, peak flow acceleration; (d) $t=0.25$, early flow deceleration; and (e) $t=0.35$, intermediate flow deceleration.

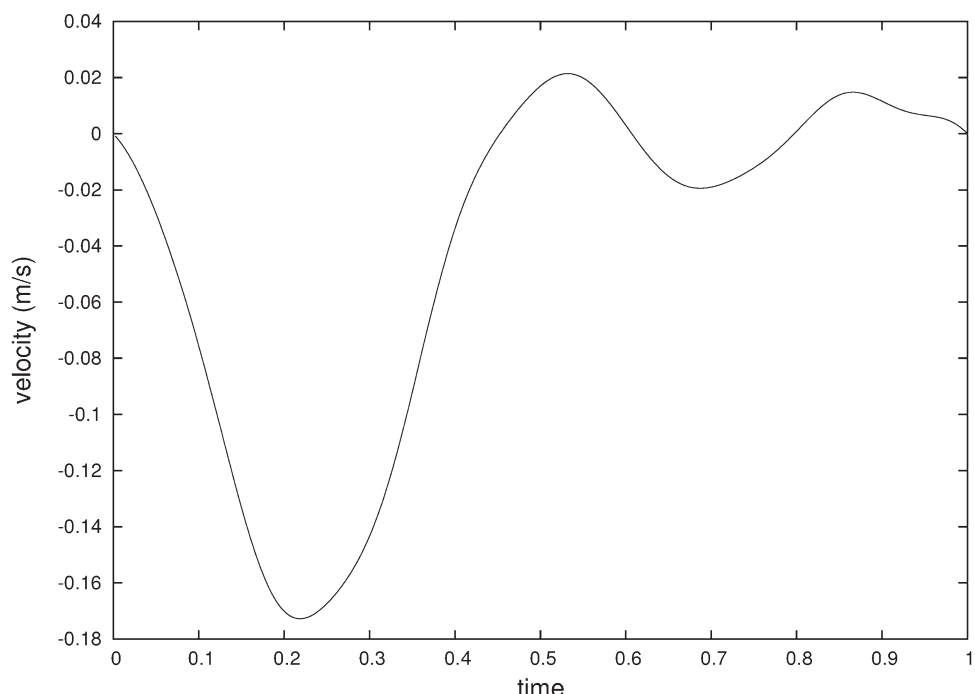
It has been shown that intracranial aneurysms are subjected to the full force of systemic blood pressure.²⁸ Specifically, mean intra-aneurysmal blood pressures equal mean systemic arterial pressure, which is pulsatile in nature. For the inlet velocity boundary condition, the flow was approximated by a fast Fourier transform to fit the intra-aneurysmal velocity field of the computer models flow cycle, such that:

$$V(t) = \frac{\mu}{5dp} \sum_{n=1}^9 (a_n \cos(2\pi(n-1)t) + b_n \sin(2\pi(n-1)t)) \quad (2)$$

Peak and mean velocities were 0.175 m/s and 0.05 m/s, respectively (eqn (2)). Corresponding, peak and mean Reynolds numbers are 700 and 200 m/s, respectively. Time steps were taken at $t=0.0025$ s, and 30 iterations per time step were performed to indicate per step convergence.

All tabulated results were calculated at five different time points: (a) $t/T=0.05$, early flow acceleration; (b) $t/T=0.15$, intermediate flow acceleration; (c) $t/T=0.225$, peak flow acceleration; (d) $t/T=0.25$, early flow deceleration; and (e) $t/T=0.35$, intermediate flow deceleration. Here, T is the period of the fluid flow. From a clinical point of view, the pulsatile flow of blood through the artery is continuous and is independent of any reference point in time. However, since the solution to the partial differential equation governing the flow of blood through the artery is dependent on the initial conditions imposed at the onset of the calculation, all profiles calculated after the solution clearly indicates that the limiting effect of transients due to initial conditions is negligible. It is well documented that finite element and finite volume techniques are severely mesh (grid) dependent.^{29–31} Hence, it is imperative that any numerical technique used to predict optimal medical procedures should be substantially accurate in their predictions. Specifically, as the grid is refined by increasing the number of points utilized during the study, the more precise become the results such as wall shear stress and velocities.

Profiles of velocity, pressure and wall shear stress were accepted at error of 0.07%.³¹ Further refinement did not significantly change the distribution of any of the variables. Once



the simulations were complete, the flow characteristics of this two-dimensional virtual model were compared with the *in vitro* three-dimensional model⁹ which measured two-dimensional velocity at the mid-plane (symmetry plane) of the ostium.

Modifications in neck and proximal dome configuration

Changes in the shape of the aneurysm neck and proximal dome were then made without affecting the size of the ostium itself. A subset of the configurations studied is depicted in figure 2. Identical simulations as above were then performed on these models and qualitative and quantitative results were obtained, comparing qualitative changes in vorticeal patterns and quantitative changes in wall shear stress, velocity and dynamic pressures along the aneurysm wall and parent artery.

RESULTS

Flow characteristics of virtual model

Flow simulation in the two-dimensional computer model was assessed at various points of the flow cycle. In early flow acceleration, uniform laminar flow is interrupted at the location of the aneurysm's proximal neck as flow propagates up into the aneurysm neck in an undulant fashion, thereafter turning down into the main lumen. Flow in the opposite direction is initiated within the aneurysm. At intermediate flow acceleration, the flow continues to propagate but is more directed to the distal neck of the aneurysm. Clockwise flow in the form of a vortex is seen at the lower distal region of the aneurysm during peak flow acceleration. During early flow deceleration, the vorticeal flow propagates up into the aneurysm as flow in the opposite direction becomes pronounced. Finally, during intermediate flow deceleration, the flow continues its vorticeal pattern within the

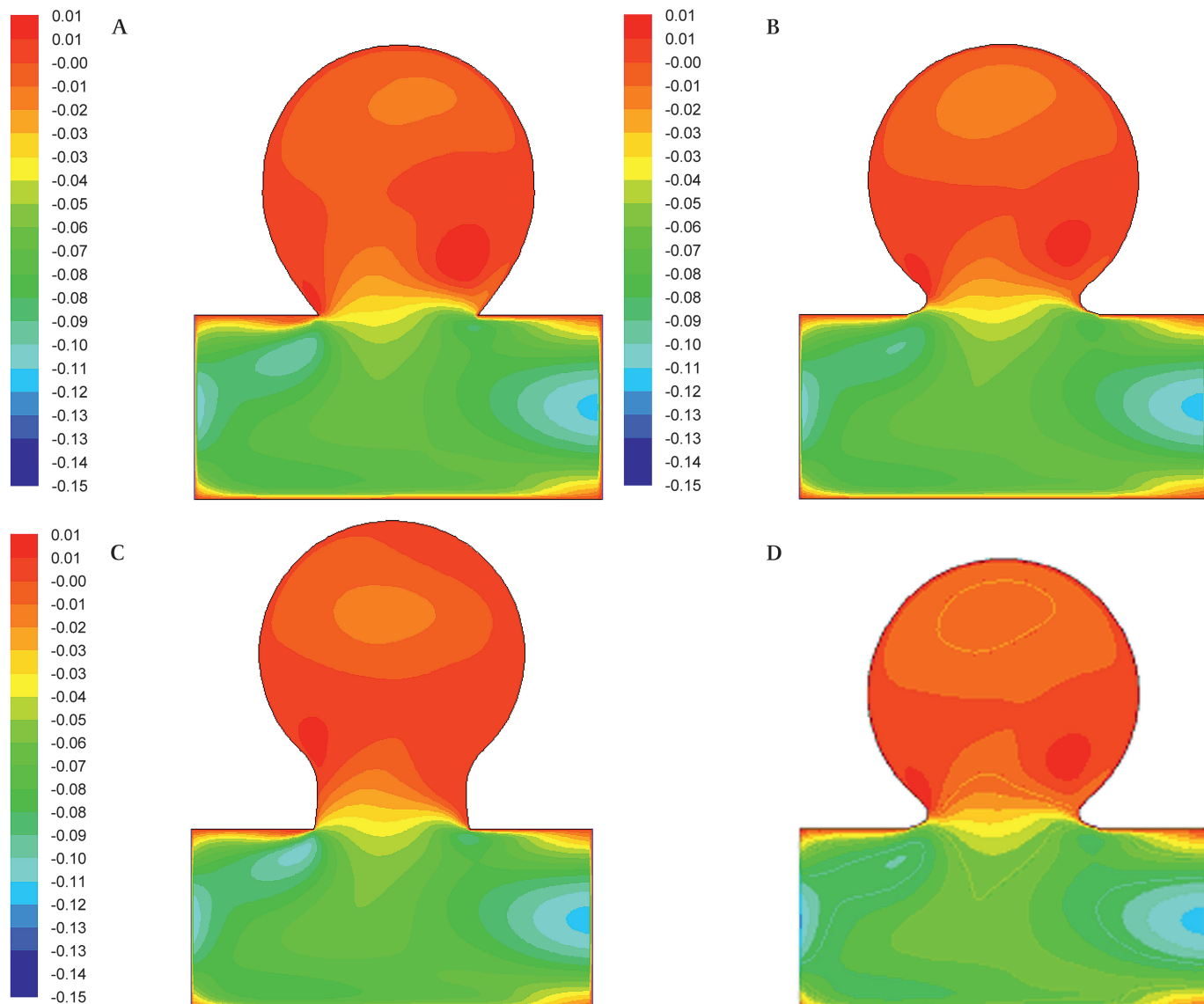


Figure 2 Variations in neck and proximal dome configuration for analysis in computer simulation model. Contours of intra-aneurysmal flow (x velocity) at time $t=0.05$ during the early acceleration phase. (A) Flow in an aneurysm with no neck. (B) Flow in an aneurysm with a small neck. (C) Flow in an aneurysm with a longer neck. (D) Actual configuration which coincides with the aneurysm of Byun and Rhee.⁹ These configurations match the progression of geometries chosen as the geometry converged to the geometry of the *in vitro* aneurysm.⁹ Note that in all instances, the dimensions of the neck and proximal dome of the aneurysm were kept constant.

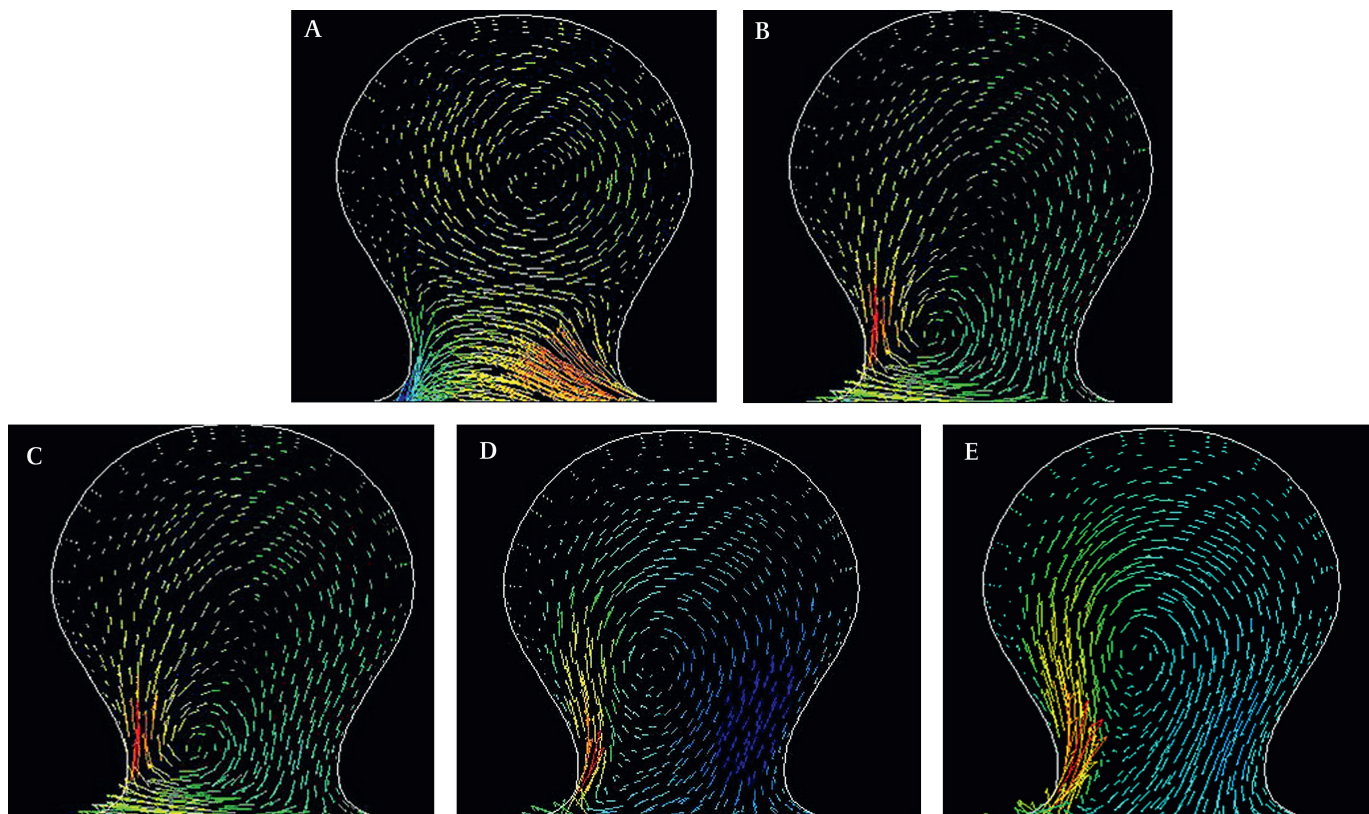


Figure 3 Flow signature for computer generated model. (A) early flow acceleration—note the interrupted laminar flow pattern at the proximal neck of the aneurysm. (B) Intermediate flow acceleration—flow within the aneurysm is noted as it propagates towards the distal neck. (C) Peak flow acceleration—a change in vortical flow pattern is noted which results in clockwise flow in the distal region of the aneurysm. (D) Early flow deceleration—vortex flow propagates to the upper portion of the aneurysm's dome. (E) Intermediate flow deceleration—note the flow continues its vortical pattern within the aneurysm.

aneurysm and turbulent flow initiates within the artery. Figure 3 depicts the flow signature for the computer generated model during (A) early flow acceleration, (B) intermediate flow acceleration, (C) peak flow acceleration, (D) early flow deceleration and (E) intermediate flow deceleration.

Validation of computer model to in vitro experimental model

Byun and Rhee reported the qualitative velocimetry profile of their three-dimensional model in two dimensions.⁹ When comparing the profiles of the published experimental data with the profiles generated by this finite volume analysis derived model, identical flow signatures were noted at the specified timed intervals of the pulse cycle. Flow velocities and the distinct sequencing of vortical flow formation were identical (figure 4).

Effects of alterations on configurations of neck and proximal dome

Shear stress involves the friction between individual blood elements or between blood elements and the vessel wall. Arterial wall shear stress essentially is the product of blood viscosity and the shear rate at the arterial wall. There is evidence that high wall shear stress appears to be a predisposing factor for aneurysm formation in healthy arteries.⁶ By selectively altering the configuration of the proximal dome and neck of the aneurysm, the effects on wall shear stress and dynamic forces were evaluated. The initial geometry consisted of a spherical aneurysm with negligible neck height (figure 2A). Subsequently, the geometry was continually altered to smooth the interface transition (of the neck) from artery to aneurysm (figure 2B-D).

Although the actual size of the ostium remained constant (3.1 mm), minimal changes in the shape of the neck and proximal dome significantly changed the flow pattern and hence the wall shear stress in the aneurysm and parent vessel.

Vortical flow patterns within the aneurysm dome changed, with flow velocities increasing at the interface between the aneurysm neck and parent vessel. The velocities at the distal neck (inflow zone) increased when proximal dome configurations were modified as well. As seen in in vitro measurements of fluid induced wall shear stress, distribution of wall shear stress was not uniform in the aneurysm walls. Numerical computations indicate a significant change in wall shear stress throughout one cardiac cycle with the highest amount of wall shear stress occurring at the distal neck of the aneurysm (figure 5).

Quantitatively accurate three-dimensional simulations

When a model of a three-dimensional phenomenon is approximated in two dimensions, one is left to wonder what is lost in the simplification. Hence a three-dimensional numerical model was rendered to compare the accuracy and representation of the two-dimensional results. The two-dimensional simulation produced qualitatively accurate velocity profiles. That is, after careful grid refinements and time step reductions, the two-dimensional simulations accurately represent the results obtained via the experimental in vitro model within the plane of analysis. However, further work is necessary to determine what characteristics, if any, are neglected when two-dimensional simulations are used to model three-dimensional phenomena.

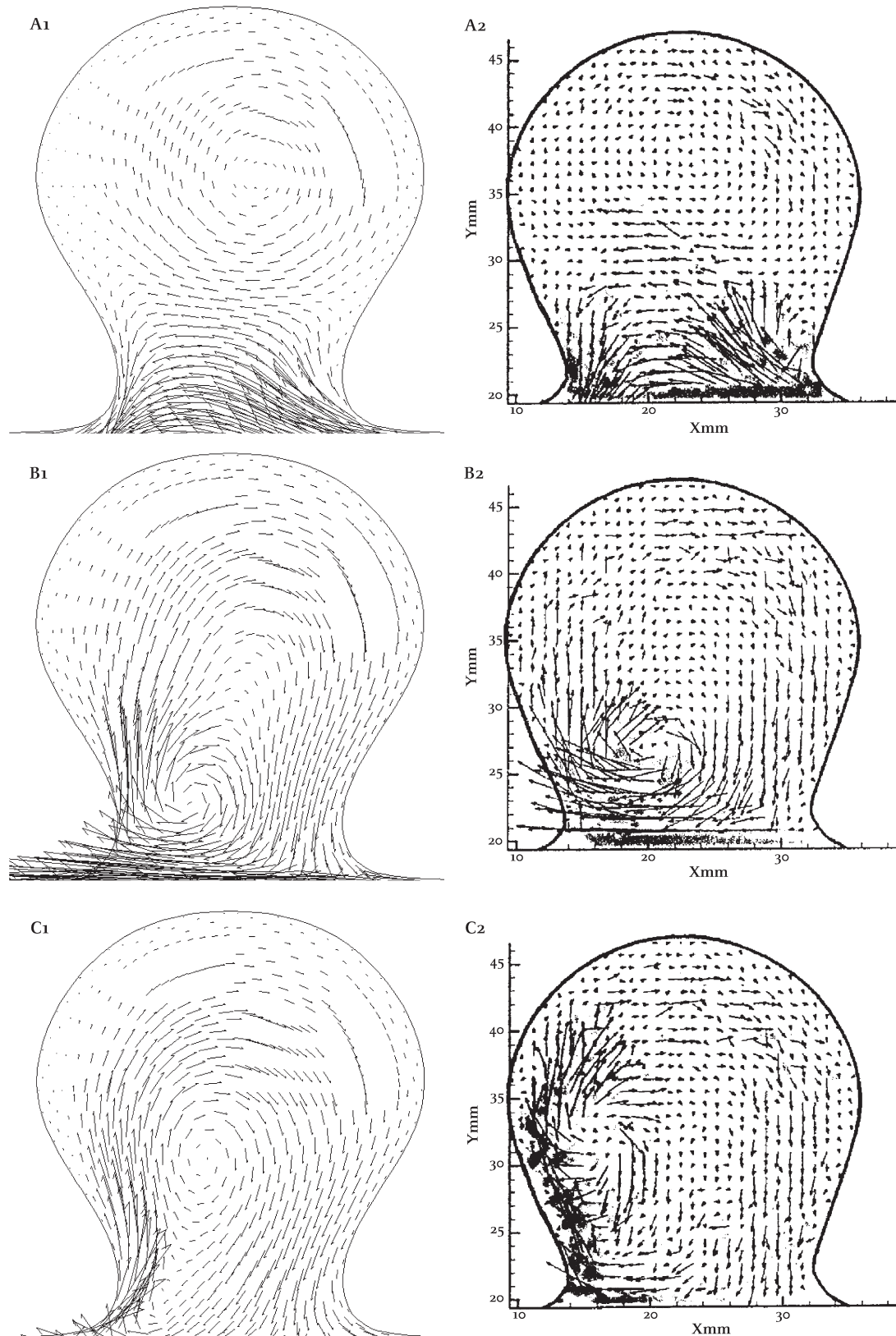


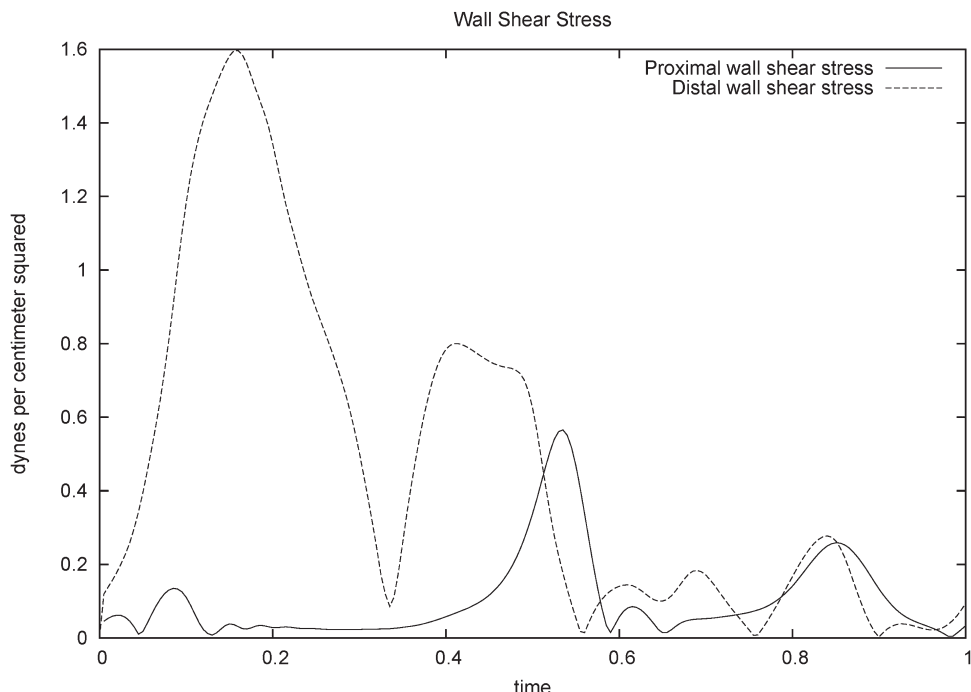
Figure 4 (A–C) Intra-aneurysmal velocity fields at different phases of a flow cycle in an aneurysm model. Flow direction in the parent artery is from right to left. The left column (A1, B1 and C1) depicts the velocities obtained via finite element method, corresponding to phases (B–D). The right column (A2, B2 and C2) depicts velocities obtained in the in vitro experimental model,⁹ also at phases (B–D). The profiles agree qualitatively.

DISCUSSION

The mechanisms which precipitate the rupture of cerebral aneurysms have not been fully elucidated. Although some evidence exists as to which factors might predict rupture, clin-

ical experience constantly reminds us that the ideal predictive model for aneurysmal rupture does not yet exist.^{1–4} Aneurysm size has been shown to be a very important parameter in predicting aneurysm rupture. Aneurysm location and the

Figure 5 Plots of wall shear stress for one cardiac cycle at the proximal and distal neck of the aneurysm.



presence of irregularities (blebs) have also been shown to be important in predicting rupture when using multivariate analysis. Indeed, various mathematical relationships such as aneurysm volume to neck surface area seem to predict which aneurysms might be prone to thrombosis.^{32,33}

Successful modeling of aneurysms to study their behavior and ultimately predict which are at risk of rupture can be very expensive if bench top synthetic models are to be used. As suggested by the results of our present study, such models would require multiple iterations of an aneurysm with minor changes in shape as a means of testing how each modification affects wall shear stress and other hemodynamic forces. Thus the detriment to bench top synthetic models is that conclusions drawn from such studies would be limited to aneurysms of very similar configuration and size, and could thus not be generalized to the entire population at risk. Furthermore, all conclusions are qualitative in nature unless further, more expensive, modifications are added to the model.

Computer modeling of aneurysms has the advantage of allowing multiple configurations of aneurysms to be assessed at relatively lower cost. Previous computer simulations were limited by the degree of complexity that could be introduced into the model and thus the validity of such models was questioned. The present study directly addresses these aforementioned issues. Firstly, by replicating an experimental model of a published silicone aneurysm and simulating the input flow profile, this study demonstrated that the results of our model are qualitatively identical to the bench top model. Secondly, important additional information such as wall shear stress and dynamic pressure can be gleaned from this computer generated model information not readily available by assessing flow characteristics with particle velocimetry used in experimental model. Furthermore, by changing the aneurysm neck's configuration independently of any alterations in neck size, significant changes in wall shear stress, dynamic forces and flow signatures were noted. To the best of our knowledge, this finding represents the first time that such small changes in the shape of the transition zone of an aneurysm has been shown to make such significant changes in hemodynamic patterns.

Flow signature

Although particle velocimetry provides an excellent visual, qualitative analysis of the flow dynamics within the aneurysm and parent vessel, it does not directly demonstrate the forces being experienced at various locations along the aneurysm and its parent vessel. By creating a computer model with identical flow signatures to the published experimental model, formal analysis of pressure, wall shear stress and other factors can be objectively quantified at any stage of flow along any segment of the model. For example, dynamic pressure was computed at intermediate flow deceleration ($t=0.35$) for the computer generated model. Analysis of dynamic pressure along the length of the parent vessel and aneurysm is increased at the distal portion of the neck, although velocity profiles demonstrate an initial inflow zone at the proximal neck. Maximum pressure is centrally located below the aneurysm in the center of the artery.

The flow signature of the computer generated model qualitatively matches the flow signature achieved by an experimental two-dimensional analysis of a three-dimensional bench top model for a side wall aneurysm exposed to pulsatile flow. Both exhibit a significant increase in vortical flow at the distal neck of the aneurysm during the late phase of the flow cycle.

These concordant data suggest that finite volume analysis methods provide valuable information regarding the hemodynamic characteristics of side wall aneurysms. Furthermore, although this model is a simple two-dimensional flow model, the data obtained are identical to the two-dimensional representation of a three-dimensional bench top flow model. This suggests that valuable data about flow dynamics in aneurysms can be obtained with relatively simple models.

Changes in neck configuration

Neck size has been shown to be an independent predictor of aneurysmal regrowth and recurrence after endovascular treatment.³⁴ However, the actual configuration of the transition zone between the parent artery and the dome of the aneurysm has not been studied. This study describes the finding that differences in the shape of the transition zone plays a significant role in the flow dynamics within the parent artery. As demonstrated in figure 2, a

sharp transition zone between the aneurysm and parent artery results in an increase in flow inside the aneurysm itself. As the transition zone changes to a smoother configuration (less acute angulation between parent artery and aneurysm), not only is there a demonstrable change in the flow signature, but there is a significant change in wall shear stress and dynamic pressures. Such differences may be important contributors to aneurysm growth, rupture and potential recurrence after treatment.

Although this model is limited by its two-dimensional analysis, we believe this numerical technique to be an improvement over the current use of clear acrylic aneurysm models analyzed via particle imaging velocimetry.^{9–32} The authors as well as other researchers are currently employing three-dimensional CFD analysis.^{20–25,32} An additional limitation of the model is that the artery is represented a rigid tube. For example, Shojima *et al* determine the magnitude and role of wall shear stress on cerebral aneurysm using finite element analysis with the assumption of Newtonian fluid property for blood and the rigid wall property for the vessel and the aneurysm as used in this work.³⁵ Proper representation of the arterial/aneurysmal blood flow phenomenon is a very pernicious problem which involves the Navier-Stokes equation governing the time dependent flow within an artery adjoined to the cerebral saccular aneurysm, elasticity to model the radial wall motion of the vessel and the aneurysm ostium, the dissipative response of human tissue and time dependence on hardening/recovery of tissue. Lastly, any biomechanical analysis cannot take into account hemodynamic factors such as thrombosis.

Clinicians and scientists from a variety of different fields have applied their expertise and explored this problem from their respective points of view. They have thus begun to glean isolated information on how aneurysms develop and rupture. What experimental science is in need of is a non-invasive method which predicts blood flow characteristics and the potential of aneurysm growth and rupture. A better understanding of why certain aneurysms recur, whether it is by progressive growth of abnormal tissue at the neck of the aneurysm or the change in the configuration of the platinum coils within an aneurysm, is vital to determining which lesions might be best treated through surgical clipping or endovascular coiling. Hassan *et al* applied CFD analysis to assess three-dimensional digital subtraction angiography findings in a patient with a giant vertebrobasilar aneurysm to simulate and compare the consequences of left and right vertebral artery occlusion.³⁶ Steinman *et al* used CFD analysis combined with computed rotational angiography to study the hemodynamics of blood flow in a giant carotid-posterior communicating artery aneurysm that was subsequently coiled.²³

The decision to treat unruptured intracranial aneurysms is never taken lightly. Irrespective of the modality of treatment, substantial morbidity can result from complications of micro-surgical or endovascular approaches. These complex lesions vary in size, shape, location and other biophysical and rheological parameters that complicate the ability to predict development, growth, rupture and indeed recurrence of these often devastating lesions. Of the numerous characteristics that have been studied as a means of predicting rupture, aneurysm size, location and presence of irregularities on the aneurysm seem to be the strongest predictors. Other features may be equally important, although less measurable. Genetics, the various biological properties of the tissue and its response to mechanical (flow related) stress have been studied and are currently being modeled. Consequently, progress in understanding the natural history of aneurysms is hampered by the complex interaction of these factors and the inability to adequately study these lesions *in vivo*.

CONCLUSION

Using finite volume analysis, a two-dimensional model has been developed to assess flow characteristics in saccular cerebral aneurysm. The results agree very well with *in vitro* clinical studies. Our model also predicts shear stresses and pressure distribution at five different phases of a flow cycle in different neck and dome configurations. In this study, we have demonstrated that careful two-dimensional finite volume analysis modeling of side wall aneurysms can faithfully reproduce the flow signatures of synthetic bench top aneurysm models. In addition to the previously demonstrated association of flow characteristics with the size of the ostium, this study also indicates a dependence of the flow characteristics on the shape of the neck and dome near the neck of the aneurysm. Further development of this theoretical, non-invasive technique may lead to the prediction of aneurysm behavior, such as aneurysm regrowth after treatment.

The benefits of such computer generated models are not limited to the qualitative changes that can be readily apparent. Such relatively simple models add a dimension of quantitative results that include the ability to determine wall shear stress and dynamic pressures along any segment of the model during any phase of the flow cycle. In addition, we have shown that configuration changes in the transition zone between the aneurysm and parent vessel can substantially affect flow dynamics, independent of changes in the size of the neck. Further studies of this model may help to determine how these changes in shear stress contribute to aneurysm growth and potential regrowth. This study has validated three-dimensional aneurysmal blood flow utilizing two-dimensional CFD. Advantages of this technique include: (1) the ability to create or modify complex geometries which model actual aneurysms, (2) provide accurate predictions of flow dynamics, wall shear stress and pressure distribution and (3) yield a savings in computational time and resources over three-dimensional simulations.

Acknowledgments The authors thank the Applied Mathematics Research Center and the Departments of Mathematics, Biotechnology and Applied Mathematics and Theoretical Physics at DSU. Additionally, the authors thank the Center for Applied Mathematics and Statistics, the Department of Biomedical Engineering, the Department of Mathematical Sciences at NJIT and the Department of Neurological Surgery at UMDNJ for research facilities.

Funding This research was supported in part by DoD grant DAAD19-03-1-0375 (DAL), the National Science Foundation grant DMS 98-03605 (DAL), National Science Foundation Grant DMS 07-08977 (MS) and the Foundation at the New Jersey Institute of Technology (DAL).

Competing interests None.

Provenance and peer review Not commissioned; externally peer reviewed.

REFERENCES

- Chaudhry HR, Lott DA, Prestigiacomo CJ, *et al*. Mathematical model for the rupture of cerebral saccular aneurysms through three-dimensional stress distribution in the aneurysm wall. *Journal of Mechanics in Medicine and Biology* 2006;6:325–35.
- Di Martino ES, Budagni G, Fumero A, *et al*. Fluid-structure interaction within realistic three-dimensional models of the aneurysmatic aorta as a guidance to assess the risk of rupture of the aneurysm. *Med Eng Phys* 2001;23:647–55.
- Egelhoff CJ, Budwig RS, Elger DF, *et al*. Model studies of the flow in abdominal aortic aneurysms during resting and exercise conditions. *J Biomech* 1999;32:1319–29.
- Meng H, Feng Y, Woodward SH, *et al*. Mathematical model of the rupture mechanism of intracranial saccular aneurysms through daughter aneurysm formation and growth. *Neurol Res* 2005;27:459–65.
- Prestigiacomo CJ, He W, McIntosh T, *et al*. Predicting rupture probabilities through the application of a CTA-derived binary logistic regression model. *J Neurosurg* 2009;110:1–6.
- Tateshima S, Murayama Y, Villablanca JP, *et al*. In vitro measurement of fluid-induced wall shear stress in unruptured cerebral aneurysms harboring blebs. *Stroke* 2003;34:187–92.

7. **Wulandana R**, Robertson AM. A model of early stage aneurysm development based on an inelastic multi-mechanism constitutive equation. *Bioengineering Conference, American Society of Mechanical Engineers* 2001;**50**:42.
8. **Brands DWA**, Peters GWMM, Bovendeerd PHM. Design and numerical implementation of a 3-D non-linear viscoelastic constitutive model for brain tissue during impact. *J Biomech* 2004;**37**:127–34.
9. **Byun HS**, Rhee K. Intraaneurysmal flow changes affected by clip location and occlusion magnitude in a lateral aneurysm model. *Med Eng Phys* 2003;**25**:581–9.
10. **David G**, Humphrey JD. Further evidence for the dynamic stability of intracranial saccular aneurysms. *J Biomech* 2003;**36**:1143–50.
11. **Kumar BVR**, Naidu KB. Finite element analysis of nonlinear pulsatile suspension flow dynamics in blood vessel with aneurysm. *Comput Biol Med* 1995;**25**:1–20.
12. **Kumar BVR**, Yamaguchi T, Liu H, et al. Numerical simulation of 3D unsteady flow dynamics in a blood vessel with multiple aneurysms. *Bioeng Conference ASME* 2001;**50**:475–6.
13. **Oshima M**, Torii R, Kobayashi T, et al. Finite element simulation of blood flow in the cerebral artery. *Comput Methods Appl Mech Eng* 2001;**191**:661–71.
14. **Pedrizzetti G**, Domenichini F, Tortoriello A, et al. Pulsatile flow inside moderately elastic arteries, its modeling and effects of elasticity. *Comput Methods Appl Mech Eng* 2002;**5**:219–31.
15. **Seshaiyer P**, Humphrey JD. On the protective role of contact constraints on saccular aneurysms. *J Biomech* 2001;**3**:607–12.
16. **Shah AD**, Humphrey JD. Finite strain elastodynamics of intracranial saccular aneurysms. *J Biomech* 1999;**32**:594–9.
17. **Liou T-M**, Liou S-N. A review on in vitro studies of hemodynamic characteristics in terminal and lateral aneurysm models. *Proceedings of the National Science Council ROC (B)* 1999;**23**:133–48.
18. **Ortega HV**. Computer simulation helps predict cerebral aneurysms. Journal Articles by Fluent. New Hampshire: Fluent Incorporated, 1999: JA071.
19. **Byun HS**, Rhee K. CFD modeling of blood flow following coil embolization of aneurysms. *Med Eng Phys* 2004;**26**:755–61.
20. **Castro MA**, Putman CM, Cebral JR. Patient-specific computational modeling of cerebral aneurysm with multiple avenues of flow from 3D rotational angiography images. *Acad Radiol* 2006;**13**:811–21.
21. **Ford MD**, Stuhne GR, Nikolov HN, et al. Virtual angiography for visualization and validation of computational models on aneurysm hemodynamics. *IEEE Trans Med Imaging* 2005;**24**:1586–92.
22. **Juchems MS**, Pless D, Fleiter TR, et al. Non-invasive, multi detector row (MDR) CT based computational fluid dynamics (CFD) analysis of hemodynamics in infrarenal abdominal aortic aneurysm (AAA) before and after endovascular repair. *Röfo* 2004;**176**:56–61.
23. **Steinman DA**, Milner JS, Norley CJ, et al. Image based computational simulation of flow dynamics in a giant intracranial aneurysm. *AJNR Am J Neuroradiol* 2003;**24**:559–66.
24. **Wang QH**, Ma LT, Wu ZQ, et al. Formation and hemodynamics of pseudoaneurysm after rupture and bleeding of aneurysm: an experiment with dogs. *Zhonghua Yi Xue Za Zhi* 2005;**85**:2259–63.
25. **Yamamoto S**, Maruyama S, Nakahara Y, et al. Computational flow dynamics in abdominal aortic aneurysm using multislice computed tomography. *Nippon Hoshasen Gijutsu Gakkai Zasshi* 2006;**62**:115–21.
26. **Hademous GJ**, Massoud TF. *Hemodynamics: the physics of blood flow in the physics of cerebrovascular disease: biophysical mechanisms of development, diagnosis and therapy*. New York: Springer-Verlag, 1998:101–31.
27. **LaDisa JF, Jr**. Three-dimensional computational fluid dynamics model of alterations in coronary wall shear stress produced by stent implantation. *Ann Biomed Eng* 2003;**31**:972–80.
28. **Ferguson GG**. Direct measurement of mean and pulsatile blood pressure at operation in human intracranial saccular aneurysms. *J Neurosurg* 1972;**36**:560–3.
29. **Bayliss A**, Belytschko T, Kulkarni M, et al. On the dynamics and the role of the imperfection for localization in thermo-viscoplastic materials. *Modelling and Simulation in Materials Science and Engineering* 1994;**2**:941–64.
30. **Lott-Crumpler DA**. The formation and properties of shear bands in viscoplastic materials. *Model Simul Mat Sci Engrg* 1997;**5**:317–36.
31. **Stuhne GR**, Steinman DA. Finite-element modeling of the hemodynamics of stented aneurysms. *J Biomech Eng* 2004;**126**:382–87.
32. **Tateshima S**, Vinuela F, Villablanca JP, et al. Three-dimensional blood flow analysis in a wide-necked internal carotid artery-ophthalmic artery aneurysm. *J Neurosurg* 2003;**99**:526–33.
33. **Roach MR**. A model study of why some intracranial aneurysms thrombose but others rupture. *Stroke* 1978;**9**:583–87.
34. **Raymond J**, Guilbert F, Weill AF, et al. Long-term angiographic recurrences after selective endovascular treatment of aneurysms with detachable coils. *Stroke* 2003;**34**:1398–403.
35. **Shojima M**, Oshima M, Takagi K, et al. Magnitude and role of wall shear stress on cerebral aneurysm: computational fluid dynamic study of 20 middle cerebral artery aneurysms. *Stroke* 2004;**35**:2500–5.
36. **Hassan T**, Ezura M, Timofeev EV, et al. Computational simulation of therapeutic artery occlusion to treat giant vertebrobasilar aneurysm. *AJNR Am J Neuroradiol* 2004;**25**:63–8.